Soil & Tillage Research 261 (2026) 107193

Contents lists available at ScienceDirect

Soil & Tillage Research

journal homepage: www.elsevier.com/locate/still

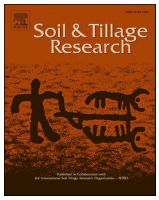

Stratified network analysis of biochar-soil systems: Structural patterns associated with greenhouse gas emission responses

Bruno Rafael De Almeida Moreira [a,*], Jinze Bai [a,b], Sudhir Yadav [a,*]

[a] Queensland Alliance for Food Innovation, The University of Queensland, St. Lucia 4072, Australia
[b] College of Agronomy, Northwest A&F University, Yangling, Shaanxi 712100, China

ARTICLE INFO

Keywords:
Complex systems
Methane
Multivariate analysis
Nitrous oxide
Soil carbon
Soil system modelling

ABSTRACT

Biochar is extensively studied as a soil amendment with potential to reduce greenhouse gas (GHG) emissions, but field trial outcomes remain inconsistent, limiting generalisable mitigation strategies. Most analyses focus on direct amendment effects, offering limited insight into predictable co-variation patterns. This study applies stratified network analysis to 55 globally distributed field trials, examining chemical, microbial, and emission variables across environmental and management contexts. Correlation-based networks were constructed within ecological strata defined by climate, soil pH, crop type, fertilisation, and trial duration. Using multiscale metrics, such as edge density, centrality, modularity, assortativity, and canonical coherence, we evaluated association patterns at global (system), mesoscopic (subsystem), and variable (local) levels. Biochar application rate, soil pH, and total nitrogen consistently occupied central positions, influencing key structural associations within biochar-soil networks. CH_4, N_2O, and microbial gene markers were more peripheral, especially under acidic or low-input conditions, suggesting context-dependent patterns. Canonical correlation analyses revealed reproducible multiscale alignment (first-variate $r = 0.9–0.95$), supporting classification into meso-dominant, global-meso, meso-local, and disjoint regimes, each with distinct structural signatures. Partial-correlation networks retained key edges under 25% data removal, indicating structural consistency under data-limited conditions. The analysis is descriptive, but it identifies contexts where emission responses are embedded in a coherent multivariate scaffold and where interpretation is limited by sparse co-reporting. It supports prioritising soil pH, nitrogen context and amendment dose in monitoring and trial reporting, alongside more standardised co-measurement. Together, these results provide a practical basis for selecting core indicators and designing trials that test network structure across sites systematically.

1. Introduction

Achieving the Paris Agreement target of limiting global warming to well below 2 °C will require both rapid reductions in greenhouse gas (GHG) emissions and large-scale carbon dioxide (CO_2) removal from the atmosphere (Masson-Delmotte et al., 2022; Muratori et al., 2020). While engineered approaches such as direct air capture and bioenergy with carbon capture and storage (BECCS) are in development, their implementation is constrained by infrastructure, energy demand, and land-use competition (Hénault et al., 2019; Khalifah and Foltz, 2024). These constraints have intensified interest in land-based mitigation strategies that are compatible with existing agroecosystems and scalable under near-term conditions.

Agricultural soils are central to this challenge. They account for an estimated 50% of anthropogenic nitrous oxide (N_2O) emissions and 11% of methane (CH_4) emissions (Jiang et al., 2019; Tian et al., 2020, 2024). These emissions are significantly influenced by microbial transformations of nitrogen and carbon and are sensitive to soil properties, moisture, nutrient availability, and land management (López-Aizpún et al., 2020; Singh et al., 2024). As a result, agricultural systems are increasingly targeted for integrated GHG mitigation, particularly in nationally determined contributions and carbon accounting frameworks.

Biochar, a carbon-rich material derived from pyrolysed biomass, has been widely investigated as a climate-aligned soil amendment. Reported effects include increased pH buffering, altered nutrient dynamics, enhanced microbial activity, and (in some settings) reductions in CH_4 and N_2O emissions (Cayuela et al., 2013; Kabir et al., 2023; Khan et al.,

* Corresponding authors.
E-mail addresses: b.moreira@uq.edu.au (B.R. De Almeida Moreira), sudhir.yadav@uq.edu.au (S. Yadav).

https://doi.org/10.1016/j.still.2026.107193
Received 31 July 2025; Received in revised form 14 March 2026; Accepted 22 March 2026
Available online 24 March 2026

2024; Lehmann et al., 2020, 2021; Liu et al., 2023). Global mitigation potential has been estimated at 2.6–10.3 Pg CO_2-equivalent per year (Weng and Cowie, 2025). However, outcomes across field trials remain inconsistent. While meta-analyses report average reductions of 13.1% for N_2O and 6.8% for CH_4, individual studies span a wide range (Bai et al., 2025; Chagas et al., 2022).

These variable outcomes are often attributed to differences in biochar feedstock, pyrolysis temperature, and application rate (Bai et al., 2019; Bolan et al., 2023). Yet inconsistencies persist even under similar amendment conditions, suggesting that the organisation of the receiving soil system may influence responses. For instance, emission reductions are more commonly observed in acidic soils, where pH buffering may be more effective, and in biologically active systems, where microbial responses to amendment are more pronounced (Kerner et al., 2023). These observations point to a broader issue: soil-biochar-emission responses may be shaped not just by amendment traits, but by emergent organisation across chemical, biological, and environmental domains.

Current approaches, including meta-analyses (Bai et al., 2025; Borchard et al., 2019) and structural equation models (Liao et al., 2025), offer useful insights into variable-level effects. However, they rely on predefined pathways and do not explicitly describe system-wide association structures. This limits their ability to account for latent association or co-variation across subsystems, a key consideration in evaluating amendment impacts and informing generalisable models.

Network analysis offers a complementary structural perspective. Rooted in systems biology and graph theory, network methods assess patterns of association across domains without assuming linearity or causality (Borsboom et al., 2021). Metrics such as modularity, centrality, and assortativity allow the internal organisation of a system to be characterised in terms of connectivity and coherence (Epskamp et al., 2012). These methods are increasingly applied in microbial ecology, metabolomics, and complex systems research (Bauwens et al., 2022; Hu et al., 2022; Yang et al., 2018) but remain underutilised in soil GHG studies, particularly across field-based datasets.

One barrier to broader adoption is the heterogeneity of biochar field studies, which differ in climate, management, soil types, and measurement scope (Schmidt et al., 2021). This variability complicates synthesis and limits model generalisation. To support scalable, climate-relevant assessment of soil amendments, methodological frameworks are needed that tolerate asymmetry, accommodate stratification, and maintain structural interpretability across diverse contexts.

This study introduces a stratified network framework for assessing system structure in biochar-amended field soils. Using 55 globally distributed trials, we construct correlation-based networks across microbial, chemical, and emission variables, stratified by environmental and management conditions. The objectives of this study are to: (i) establish a reproducible method for network-based analysis of complex field datasets; (ii) identify structural features aligned with observed CH_4 and N_2O responses; and (iii) explore how network metrics can inform variable selection, model design, and monitoring strategy.

Rather than modelling process dynamics directly, this framework characterises how system components are organised within and across contexts. In doing so, it provides a structural layer of interpretation that complements process-based models and supports design of association-sensitive diagnostics.

By avoiding assumptions of uniformity and resisting premature generalisation, this approach reduces the risk of inconsistencies and artefactual models being carried forward across studies, an important consideration as biochar practices is evaluated for climate mitigation and incorporated into long-term monitoring strategies.

2. Materials and methods

2.1. Literature review and study selection

A systematic literature review was conducted following PRISMA guidelines (Liberati et al., 2009) to identify peer-reviewed field studies examining biochar effects on soil properties and GHG emissions. Searches were performed in Scopus and Web of Science (2000–2024) using Boolean combinations of amendment terms ("biochar", "pyrolysed biomass"), outcome terms ("N_2O", "CH_4", "microbial biomass"), and experimental descriptors ("field experiment"). After duplicate removal, studies were screened by title, abstract, and full text. Greenhouse, pot, incubation, and column studies were excluded to maintain ecological and structural comparability. Eligible field trials were required to report treatment and control means, standard deviations, and sample sizes for at least one full growing season. Data were included if at least one of the following was reported: (i) soil physicochemical properties, (ii) microbial gene abundances, (iii) seasonal GHG emissions, or (iv) biochar characteristics. Studies involving co-applied amendments (e.g. compost, digestate) or modified biochars were excluded. Graphical data were extracted using WebPlotDigitizer v5.0 where needed. The final dataset included 55 field studies (Figure S1). Detailed screening procedures and criteria are reported in Bai et al. (2025).

2.2. Variable structuring and data transformation

The analysis uses two types of variables. The first type captures the biochar treatment effect on emissions and is expressed as an effect size. The second type describes the context in which that treatment effect was observed and is kept on the scale reported by each study. For effect sizes, seasonal or cumulative N_2O, CH_4, and CO_2 emissions were expressed as lnRR:

$$\mathrm{lnRR} = \ln\left(\frac{x_t}{x_c}\right)$$

where x_t and x_c are treatment (biochar) and control means, respectively. Negative lnRR values were retained as valid responses. For interpretability, lnRR values were also back-transformed to percent change (PC) relative to the control:

$$\mathrm{PC} = (e^{\mathrm{lnRR}} - 1) \times 100$$

Because PC is asymmetric at larger lnRR magnitudes, interpretation focuses on direction and magnitude rather than visual symmetry. Where studies reported zeros, an offset equal to 1% of the minimum non-zero value for that variable was applied to enable lnRR calculation. Observations were excluded from network estimation only when treatment or control means were zero or negative such that lnRR was undefined or not interpretable. These observations were retained for descriptive summaries (Hedges et al., 1999). Contextual descriptors were organised into domains for stratification and interpretation: fertiliser inputs (fertN, fertP, fertK), site soil properties (spH, bulk density, sOC, sTN), microbial indicators (amoA, nirK, nirS, nosZ), and biochar properties (bRate, bpH, bTC, bTN, pyrolysis temperature). These variables were extracted as reported and were not converted to lnRR because paired control and treatment values were not consistently available across studies and variables. They are interpreted as descriptors of trial conditions or amendment characteristics, not as treatment effects. Missing values were handled using pairwise-complete observations for correlation estimation. Reporting-driven missingness is common in multi-study field datasets and differs across domains, so values were not imputed to avoid introducing unsupported covariance structure (Morton et al., 2019). Pairwise-complete sample sizes were retained for each variable pair so that edge strength could be interpreted in the context of reporting depth. For the null-model analyses, only observed values were permuted and the original missing-data pattern was preserved. Where study identifiers were available, permutations were restricted within study blocks so that cross-variable association was disrupted without changing study composition. Dispersion estimates and sample sizes were extracted where reported for emissions, but lnRR values were not inverse-variance weighted. Variance reporting was not consistent across

studies and outcomes (Bai et al., 2025), and applying weights only where available would have changed the effective contribution of subsets of trials. The network analyses therefore use unweighted lnRRs to describe association structure, with robustness assessed through ecological stratification, threshold sensitivity, regularised estimation, bootstrap stability checks, cross-specification comparison, and missingness-preserving permutation tests (Borsboom et al., 2021; Williams, 2022). In network figures, GHG variables are shown in alphanumeric form (N2O, CH4, CO2) for label consistency.

2.3. Ecological stratification scheme

To account for environmental and management heterogeneity across field sites, studies were grouped into ecological strata using threshold criteria based on prior literature. Stratification was applied by climate zone (temperate; subtropical), mean annual precipitation ($\leq$600; >600 mm), soil pH ($\leq$6.5; >6.5), soil bulk density ($\leq$1.3; >1.3 g cm^{-3}), cropping system (wheat-maize as upland cereals; rice), pyrolysis temperature ($\leq$500; >500 °C), nitrogen fertiliser (no; yes), and trial duration ($\leq$1 year; >1 year). Thresholds for each variable were based on source metadata and ecologically meaningful boundaries established in earlier field research (Bai et al., 2025; Jia et al., 2023; Kerner et al., 2023; Schmidt et al., 2021). To ensure structural stability and comparability, each stratum was required to contain a minimum of 250 complete observations. Within strata, only variables with at least 70% data completeness were retained for analysis (Epskamp et al., 2012). This completeness rule limits interpretation based on sparsely reported variables, but it can produce differing node sets among strata. Node-level summaries are therefore interpreted within the networks where nodes are present and remain connected, and cross-context interpretation focuses on recurring structural patterns rather than one-to-one comparisons of specific nodes (Figure S2; Figures S3-S6).

2.4. Network construction and structural metrics

For each ecological stratum, undirected Pearson correlation networks were constructed from pairwise-complete correlation matrices derived from lnRR-transformed emissions together with contextual descriptors retained on their reported scales. In these networks, nodes represent ecological variables and edges represent pairwise associations among variables (Epskamp et al., 2018; Epskamp and Fried, 2018). Both positive and negative correlations were retained for interpretation (Arthur, 2025). For the thresholded topological summaries, edges were retained when the absolute correlation coefficient was $\geq$ 0.35. This value was used as the operating threshold for the main analyses because it maintained network connectivity without discarding a large share of moderate associations. Networks were analysed across topological scales (Epskamp et al., 2018). At the global (system) level, overall compactness and association structure were characterised using average path length, network diameter, edge density, and global efficiency. At the mesoscopic (subsystem) level, subsystem organisation was described using modularity, transitivity, assortativity, and local efficiency. At the local (node) level, variable prominence and positional roles were quantified using degree, strength, closeness, betweenness, eigenvector centrality, and PageRank (Yang et al., 2024). These structural descriptors were selected for interpretability in heterogeneous ecological datasets and have been widely applied in systems-based modelling (Borsboom et al., 2021). Metric definitions and computation details are provided in the Supplementary Material (Table S1). Shortest-path structure was also examined using all-pairs shortest-path distances on the thresholded graphs, with absolute edge weights converted to distances as the inverse of edge strength so that stronger associations corresponded to shorter paths (Opsahl et al., 2010). Distances were visualised as heatmaps. To keep emission direction and variability visible alongside topology, lnRR distributions for N_2O, CH_4, and CO_2 were summarised using beeswarm plots (Figures S28-S36). To make threshold dependence explicit, the same summaries were repeated across a prespecified sensitivity grid of $|r| \geq 0.20$, 0.50, and 0.70 (Table S2; Figures S37-S44; Figures S45-S52). Self-loops were excluded because they do not add information in a correlation network and can inflate connectivity and distance-based summaries (Epskamp et al., 2012). When networks contained multiple components, disconnected node pairs were treated as missing distances because path length is undefined for unreachable pairs. Because thresholded topology was summarised using absolute edge strength, signed upper-triangle heatmaps of the full correlation matrices and the thresholded adjacency matrices were also produced to retain the direction of pairwise associations for interpretation. To assess consistency among structural descriptors across scales, canonical correlation analysis (CCA) was applied to the full set of global, meso-, and node-level metrics. Metric definitions, computation methods, and references are provided in Table S1.

2.5. Network visualisation and community structure

Visualisation of each network was conducted using the Fruchterman-Reingold force-directed layout algorithm, which improves visual interpretability in mid-sized networks by optimising edge separation and node dispersion (Fruchterman and Reingold, 1991). Nodes were scaled according to eigenvector centrality in the thresholded networks and according to overall connection strength in the regularised EBICglasso networks to highlight topological prominence. Community structure was identified using the Fast Greedy modularity algorithm, which clusters densely interconnected nodes into communities. To further characterise node roles across domains, the CONCOR (convergence of iterated correlation) algorithm was applied to generate blockmodels, grouping nodes with similar structural-equivalence profiles. This role-based classification enabled simplified representations of multi-domain associations (Borsboom et al., 2021). Outputs for topology, community partitions, role-equivalence groupings, and sign-aware association heatmaps are provided in the Supplementary Material, together with a pooled reference encoding (Figure S2; Figures S7-S10; Figures S11-S18).

2.6. Network reproducibility and structural reliability

In addition to thresholded correlation networks, regularised partial-correlation networks were estimated using EBICglasso as a complementary conditional-dependence benchmark. The main regularised model used $\gamma = 0.50$, which supports parsimonious conditional graphs and is commonly used in exploratory settings where sample size is moderate relative to the number of variables and missingness yields uneven pairwise information (Epskamp and Fried, 2018; Williams, 2022). EBICglasso estimates a sparse inverse-covariance model, reported here as a partial-correlation network. This regularisation acts on the covariance structure of the variables and is distinct from inverse-variance weighting of lnRR observations, which would weight effect sizes by their sampling variances. Estimator sensitivity was assessed by re-estimating EBICglasso networks at $\gamma = 0.20$, 0.35, and 0.75. Bootstrap-based reproducibility was assessed within each ecological stratum using 1000 nonparametric bootstrap replicates of the EBICglasso models. These resamples were used to estimate variation in partial-correlation edge weights and node strength. A case-dropping bootstrap was then used to evaluate how strongly node-strength rankings were preserved as observations were progressively removed (Figures S22-S27). Stability was summarised using the correlation stability coefficient for node strength (CS-strength), with CS-strength $\geq$ 0.25 treated as acceptable for exploratory inference in this heterogeneous, partially observed setting (Epskamp, 2020; Epskamp and Fried, 2018; Golino and Epskamp, 2017). Robustness across thresholds and estimators was summarised using pairwise Jaccard overlap of non-zero edge sets, Spearman correlations of shared edge magnitudes, Spearman correlations of node-strength rankings, and overlap among

the top five nodes by strength. Edges retained in at least 80% of specifications and with consistent sign were classified as stable, whereas edges appearing only under more permissive thresholds or within one estimator family were treated as threshold-dependent or estimator-sensitive (Epskamp and Fried, 2018; Williams, 2022). Node-level patterns were interpreted in the same way, with emphasis on variables that repeatedly occupied top-strength positions across specifications. In addition, a separate missingness-preserving permutation null model was used to test whether the observed structure exceeded that expected under random association given the available sample size and reporting pattern. Observed values were shuffled within each variable while preserving marginal distributions and the original missingness mask; where study identifiers were available, permutations were restricted within study blocks, otherwise they were conducted across the full stratum (Epskamp, 2020). Summaries, including edge count, edge density, largest connected component size, modularity, and mean absolute association strength, were compared with the corresponding null distributions to obtain empirical p values. This allowed robustness to be assessed not only in terms of resampling variability, but also against an explicit random-association benchmark. All analyses were performed in R (v4.5.2) using the packages bootnet, qgraph, igraph, concorR, Matrix, pheatmap, ggbeeswarm, and related visualisation and export tools.

3. Results

3.1. System-level topology

Network topology varied systematically across environmental, physical, and management strata (Fig. 1; Figures S2-S6). In high-rainfall environments, networks exhibited shorter average path lengths (mean = 0.9), higher global efficiency (1.5), and elevated transitivity (0.8). By contrast, networks from low-rainfall conditions showed longer average paths (1), reduced efficiency (1), and lower transitivity (0.7), consistent with more fragmented configurations (Table S2).

Soil pH strata showed marked structural contrasts. Alkaline soils yielded higher edge density (0.6), increased global efficiency (1.8), and disassortative mixing (r = -0.1), whereas acidic soils showed lower density (0.2), longer average paths (1.0), and positive assortativity (r = 0.15). Bulk density further stratified network structure: high-bulk-density networks featured shorter paths (0.8), greater edge density (0.4), and negative assortativity (r = -0.15), while low-density soils produced sparse and segmented networks (Figure S4).

Management conditions and biochar characteristics also corresponded to distinct topological configurations (Figure S5). Upland cereal networks exhibited high edge density (0.6), transitivity (0.8), and moderate disassortativity (r = -0.15). Rice-based systems had lower global efficiency and more negative assortativity (r = -0.3). Fertilised treatments showed elevated transitivity (0.9), while unfertilised treatments had lower density (0.55) but wider inter-domain linkages. Biochar pyrolysis temperature influenced structure: high-temperature treatments produced shorter paths and higher efficiency, whereas low-temperature treatments showed greater assortativity and more modular configurations (Figure S6).

Trial duration corresponded with clear shifts in global topology. Short-duration networks exhibited lower edge density (0.2), reduced global efficiency (0.8), and positive assortativity (r = 0.2). Longer-duration trials were associated with shorter paths (0.8), higher efficiency, and negative assortativity (r = -0.2), indicating more integrated connectivity.

3.2. Subsystem-level structure

Subsystem structure, assessed through modularity and cross-domain connectivity, differed systematically across environmental and management conditions (Fig. 2; Figures S7-S10). Networks from alkaline soils, high-precipitation environments, upland cropping systems, and

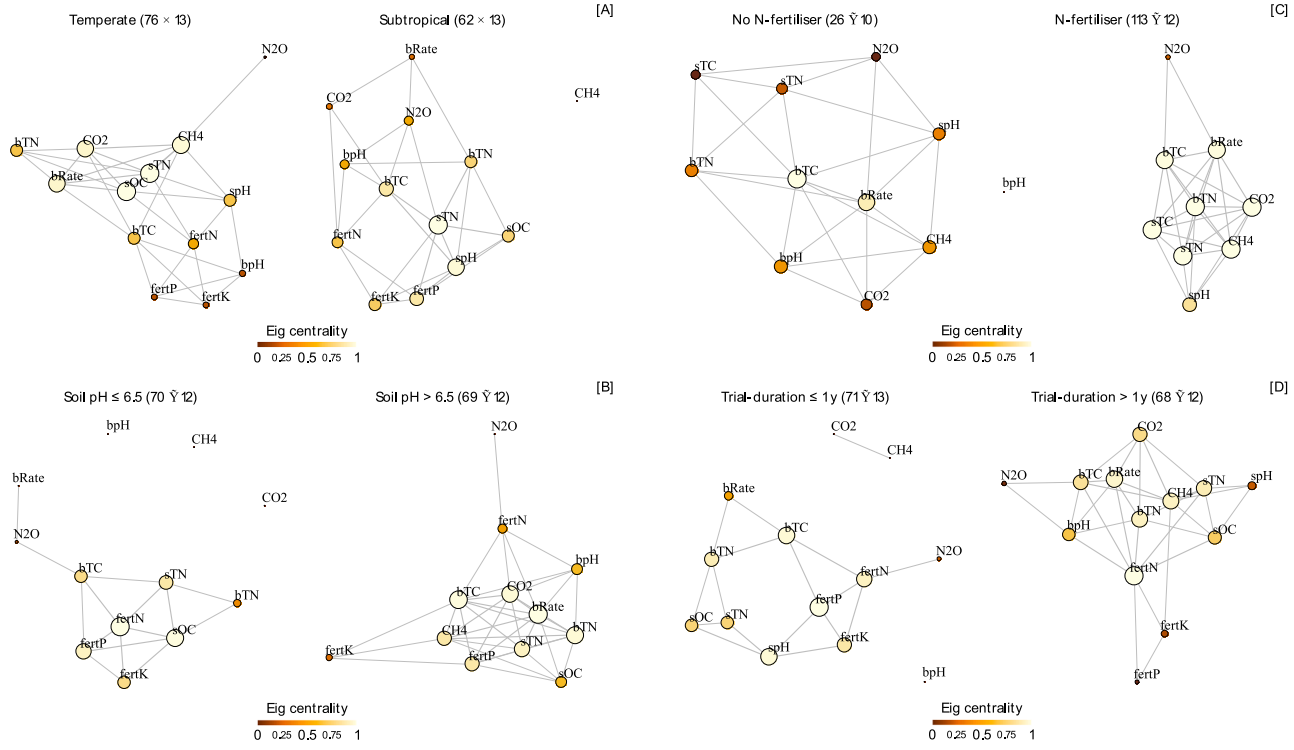

Fig. 1. Spatial arrangement and centrality gradients in stratified association networks. (A) Climate, (B) soil pH, (C) N-fertiliser, and (D) trial-duration strata shown at $|r| \geq 0.35$. Nodes represent lnRR variables and edges represent retained Pearson correlations. Positions follow a force-directed layout. Node size and shading scale with eigenvector centrality, with lighter shading indicating higher values. Parentheses give the data-matrix size (rows × columns) for each stratum. The same operating threshold and stratum order are used in subsequent network figures.

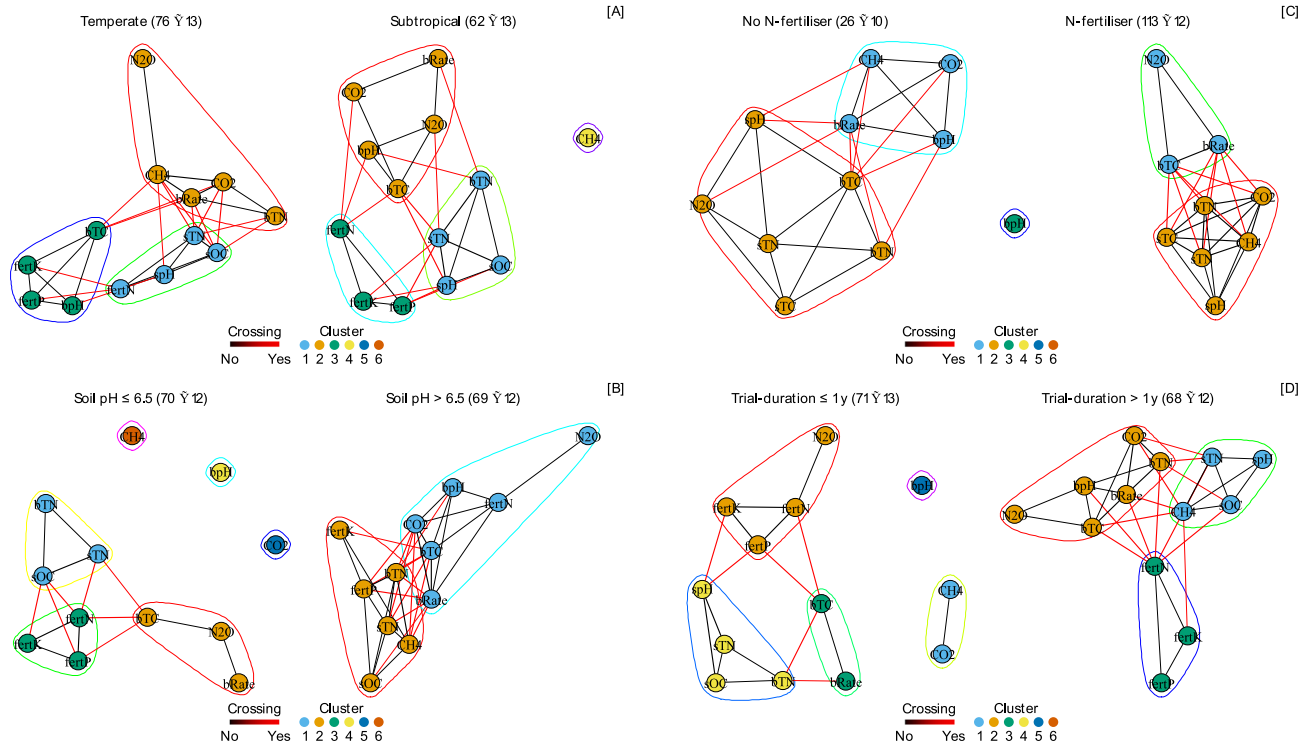

Fig. 2. Structural groupings and cross-community links in stratified association networks. Node colour marks communities detected by fast-greedy modularity. Black edges join nodes within communities, and red edges join nodes across communities.

longer trials showed elevated modularity scores and frequent inter-module linkages. In these strata, variables representing biochar application rate and total nitrogen were more frequently positioned at the boundaries between modules, indicating their structural proximity to multiple subsystems.

In contrast, acidic soils, rice-based systems, and short-duration trials were associated with lower modularity and more tightly clustered subsystems. In these configurations, biochar-related variables remained

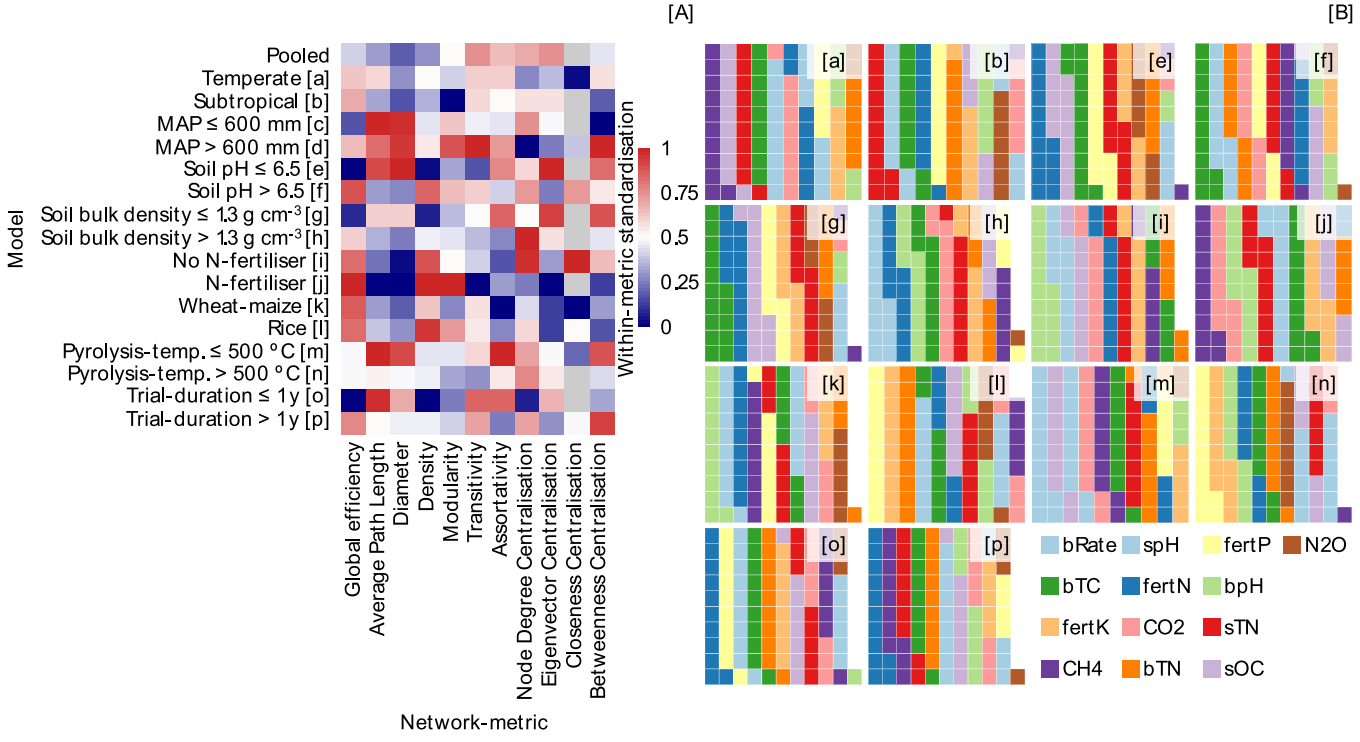

Fig. 3. Network-metric profiles and node-level influence across stratified association networks. (A) Standardised network-metric values for the pooled network and each stratum-specific network (rows) across metrics (columns). (B) PageRank distributions within each network shown as waffle plots, with each cell representing 1% of total PageRank and variables ordered by PageRank rank.

embedded within chemical modules, with fewer inter-module connections.

Cross-domain association was further quantified using crossing rate metrics (Table S3). Alkaline soils, fertilised treatments, and high-temperature biochar networks showed relatively higher crossing rates (0.4–0.5). By comparison, acidic soils, short-duration trials, and low-temperature biochars yielded lower crossing rates (0.1–0.25). Biochar-related variables exhibited higher crossing proportions (≥0.8) in wetter and fertilised conditions, while remaining more isolated (≤0.5) under dry or nutrient-limited conditions.

Blockmodelling analysis confirmed modular structure across all networks but revealed context-specific variation in module composition (Figures S11-S18). Nutrient variables, including fertiliser nitrogen, phosphorus, and potassium, consistently co-clustered in temperate environments. In subtropical conditions, these variables formed alternate modular affiliations. Greenhouse gas variables such as CH_4 and N_2O also changed modular membership across precipitation, pH, and fertilisation strata.

3.3. Node-level centrality and connectivity

Node-level analysis identified a subset of variables that consistently ranked high across centrality metrics (Fig. 3; Table S4). Biochar application rate, biochar total nitrogen, and soil pH exhibited elevated values across degree, eigenvector, betweenness, and PageRank metrics in multiple strata. These features were frequently situated in positions with broad structural reach, connecting multiple components of the network.

Peripheral variables exhibited lower centrality scores and fewer cross-subsystem connections. Biochar pH and CH_4 frequently appeared at network margins, with low betweenness and PageRank scores. Nitrogen-cycling gene markers, including amoA, nirK, and nosZ, demonstrated context-dependent centrality. In wetter conditions, amoA and nirK were positioned closer to the network centre, while in drier conditions, amoA and nosZ displayed lower centrality and reduced linkage to other domains.

Node strength further clarified patterns of connectivity. Soil organic carbon and soil pH maintained high strength scores across most ecological strata. Biochar total carbon and pH also demonstrated elevated node strength in several management and amendment conditions. These variables were characterised by a greater number of high-magnitude connections relative to others.

Cropping systems and trial duration influenced centrality distributions. In upland cereal systems, biochar application rate and pH ranked highest across multiple metrics. In rice-based systems, centrality scores were more evenly distributed across nutrient-related variables. Networks from short-duration trials showed centralisation around soil chemical variables, while longer-duration networks yielded higher centrality scores for amendment-related and emission variables, including N_2O and CH_4.

These centrality patterns were also the ones that persisted when thresholds and estimators were varied. Soil total nitrogen was the most consistently retained central node across the pooled and context-specific analyses, often alongside biochar total carbon and soil pH variables. By contrast, rice and short-duration trials showed the least stable node rankings and did not retain a consistently top-ranked node across specifications.

3.4. Multiscale structural coherence

Multiscale coherence was assessed through canonical correlation analysis across global, subsystem, and node-level structural metrics (Fig. 4). First-variate correlations indicated high alignment between structural levels, with values of 0.9 (global-meso), 0.95 (global-local), and 0.95 (meso-local) (Table S5).

Based on the sign patterns of each triplet of canonical coefficients (C_{12}, C_{13}, C_{23}), coherence regimes were identified across strata: meso-

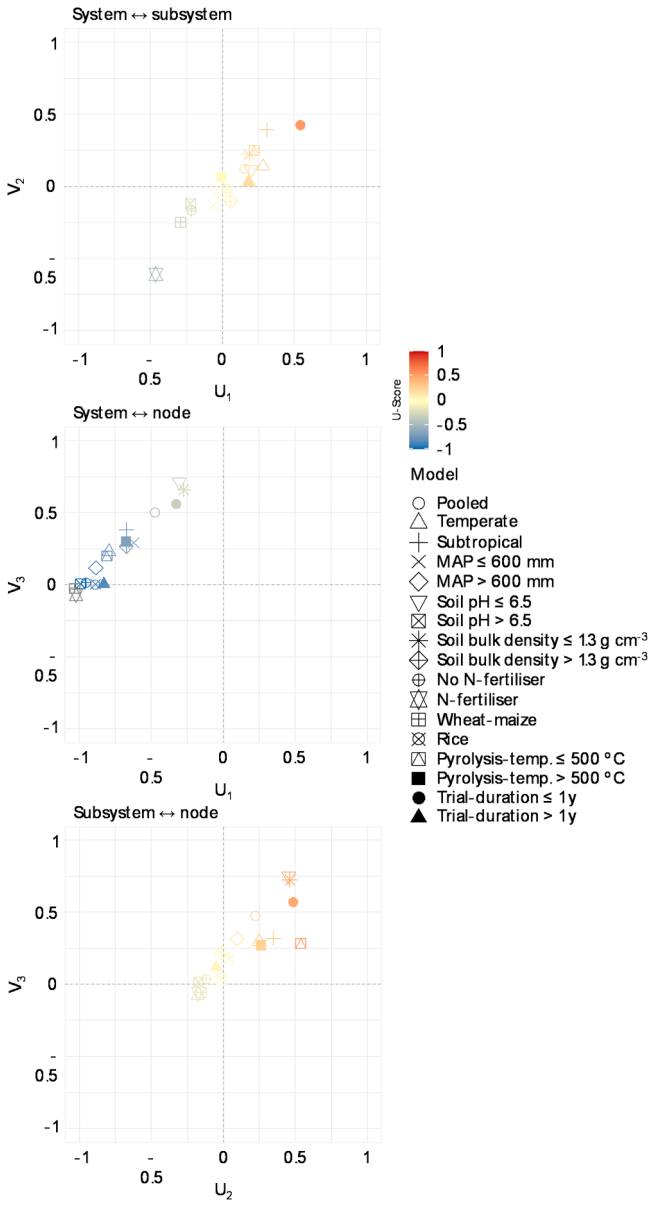

Fig. 4. Cross-scale coherence from canonical projections of paired metric blocks. (A) System versus subsystem metrics, (B) system versus node metrics, and (C) subsystem versus node metrics. Points represent the pooled and stratum-specific networks plotted by standardised canonical scores for each metric block. Colours denote the signed canonical score (U), from negative (blue) to positive (red).

dominant (+, –, +), global-meso only (+, –, –), meso-local only (–, –, +), and fully disjoint (–, –, –) (Table S6). Meso-dominant regimes were most frequently observed in alkaline soils, fertilised treatments, and longer-duration trials. Global-meso coherence appeared in rice-based systems and high-bulk-density soils. Meso-local configurations were more common in high-temperature biochar treatments and low-precipitation environments. Fully disjoint regimes predominated in unfertilised and upland cereal networks.

Metric contributions to coherence varied by axis. On the global-meso axis, canonical loadings were highest for edge density, transitivity, and global efficiency. Global-local alignment was most strongly associated with eigenvector centrality, edge density, and global efficiency. On the meso-local axis, eigenvector centrality and assortativity had the largest canonical contributions, followed by transitivity and betweenness. Average path length, modularity, and degree contributed minimally to

alignment across all axes.

These results summarise how consistency across scales is expressed topologically and quantify which structural metrics contribute most to observed coherence patterns.

3.5. Edge-level stability and network reproducibility

Edge-level stability was evaluated using regularised partial-correlation networks with bootstrapped resampling (Fig. 5; Figures S19-S21). In several ecological strata, including subtropical conditions, acidic soils, alkaline soils, and high-bulk-density contexts, partial-correlation models retained reproducible edges linking biochar properties (pH, total carbon, total nitrogen) with soil variables (pH, organic carbon, total nitrogen) and greenhouse gas emissions, particularly N_2O.

In strata defined by temperate climates, the absence of nitrogen fertilisation, or variable pyrolysis temperature, fewer partial edges were retained across bootstrap replicates. These strata exhibited lower edge counts and reduced edge-weight stability. Partial-correlation models in these conditions were more likely to yield weaker or less regular conditional structure.

Case-dropping bootstrap analyses (Figures S22-S27) showed the same broad pattern. Node-strength rankings were most stable in the denser, better-connected strata and less stable in rice, short-duration, and some high-rainfall networks. More integrated networks therefore provided a firmer basis for ranking node importance, whereas fragmented or weakly connected networks were more sensitive to model specification and data perturbation.

A broader comparison across thresholds and estimators pointed to a shared structural backbone (Table S7). Within thresholded networks, median edge-set overlap remained high across the sensitivity grid (Jaccard 0.5–0.9), and node-strength rankings were also strongly preserved (Spearman 0.7–1). EBICglasso networks showed similarly high internal consistency (edge-set Jaccard 0.7–1; strength-rank Spearman 0.8–1). Agreement between thresholded and EBICglasso networks was lower (edge-set Jaccard 0.4–0.7), showing that these approaches recovered the same broad scaffold but differed mainly in weaker or more indirect associations.

That recurring scaffold was centred on soil nitrogen, soil acidity, fertiliser descriptors, and biochar carbon or dose, which repeatedly appeared as stable nodes or edges across pooled and context-specific models. By contrast, several gas-gas links, selected microbial links, and a subset of weaker biochar-emission associations were more often threshold-dependent or estimator-sensitive. Missingness-preserving permutation tests led to the same conclusion from a different angle. In every stratum, mean absolute association strength, edge count, and edge density exceeded null expectations. The recovered backbone therefore appears stronger than would be expected from reporting pattern and sample size alone, even though weaker peripheral links remain more model-sensitive.

4. Discussion

4.1. Key findings from stratified association networks

Most syntheses of biochar field trials focus on mean effects and moderator tests. That work is well suited to estimating average N_2O, CH_4, and CO_2 responses, but it gives limited visibility on how emission effect sizes sit alongside the soil, fertiliser, and biochar descriptors that are co-reported in the same studies. The stratified network framework used here addresses that gap by examining how those variables are organised within the same multivariate structure, and how that structure shifts across ecological contexts.

In some strata, the retained associations form a connected backbone that keeps most nodes mutually reachable through short paths. In other strata, the thresholded structure fragments into multiple components,

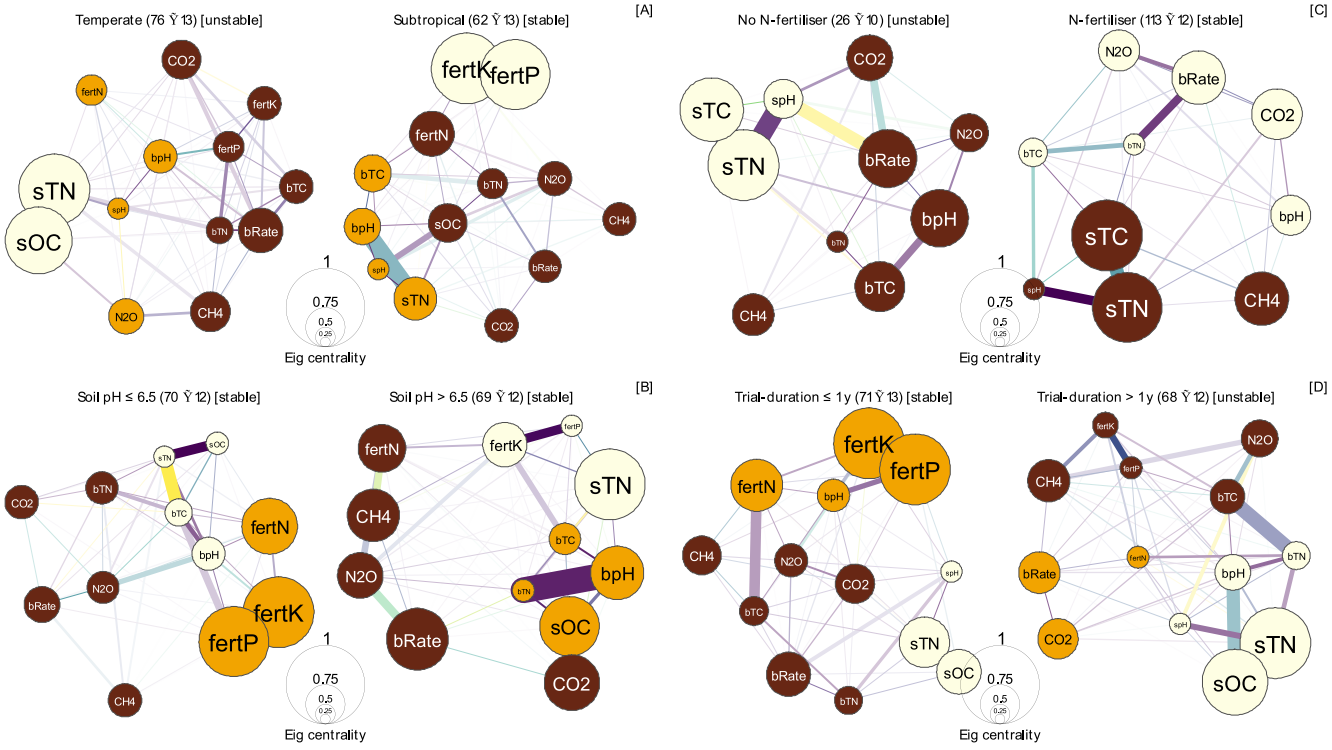

Fig. 5. Conditional association structure in regularised partial-correlation networks. Networks show conditional associations estimated from penalised precision-matrix models (EBICglasso; EBIC = 0.5). Edges appear only when present in ≥ 70% of 1000 bootstrap resamples, with thickness proportional to partial-correlation magnitude. Parentheses give the data-matrix size (rows × columns). Square brackets classify networks as stable or unstable based on case-dropping edge stability ($CS_{edge} \geq 0.25$).

leaving many node pairs unreachable. This matters because fragmentation changes what can be interpreted from network-scale summaries. When the network is partly disconnected, distance-based metrics and node centralities describe the connected portion of the graph, and they become conditional on which variables are retained and linked in that stratum.

Across strata, a narrow set of descriptors repeatedly sits in well-connected regions when available, particularly soil pH, nitrogen-related variables, and biochar dose. Emissions and microbial gene markers show less consistent placement, which is compatible with true context dependence but also with uneven measurement and uneven pairing with the core descriptors. Regularised partial-correlation estimation and bootstrap diagnostics narrow the set of associations that persist after conditioning and under resampling, providing a stability-oriented basis for prioritising candidate relationships for follow-up (Epskamp and Fried, 2018). This does not convert associations into mechanisms, but it helps distinguish edges and node positions that are consistent to modelling and sampling perturbation in a heterogeneous evidence base (Borsboom et al., 2021).

These networks are best read as descriptions of structured co-variation. Correlation-based edges and topology do not, on their own, establish ecological coupling, coordination, or causal vulnerability. Read in that way, the main result is not a fixed edge set repeated in every stratum, but a recurring multivariate scaffold that persists across reasonable specifications. Soil nitrogen, soil acidity, fertiliser context, and biochar carbon or dose repeatedly anchored that scaffold, whereas several gas-gas, microbial, and weaker biochar-emission links shifted with thresholding or regularisation. This makes the central backbone the part of the network that is most likely to travel across contexts, while the periphery remains more contingent on study composition, reporting depth, and model choice.

4.2. Implications for field trials

Interpretability depends as much on evidential strength as on edge magnitude. In literature-compiled datasets, sample size is not a single number. Under pairwise complete estimation, each edge is supported by the number of joint observations available for that variable pair within that stratum, and that joint coverage can vary widely across edges. As a result, a large edge weight does not necessarily imply compelling evidence for edge presence, and an absent edge does not necessarily imply evidence of absence. Both can reflect limited joint coverage, sampling variability, and the effects of thresholding or regularisation (Epskamp et al., 2012). For biochar field trials, this argues for reporting practices that increase joint coverage for the relationships that are most frequently interpreted.

For monitoring programmes and future trial design, the results support a staged measurement set that makes cross-site comparison feasible before adding specialised indicators. A minimal core set that is consistently measured and reported, with dispersion and sample size, would include emissions in both control and biochar treatments to support effect sizes; soil pH and at least one nitrogen context indicator; and biochar dose and key biochar properties. This aligns with the way heterogeneous biochar outcomes are commonly interpreted in meta-analysis and field agronomy, where soil acidity, nitrogen context, and application rate recur as central moderators (Bai et al., 2025). The additional point from a network perspective is that these descriptors form a recurring multivariate scaffold in the co-reported data. Microbial gene markers are most interpretable when they are collected alongside that scaffold, rather than in isolation, because the scaffold anchors cross-site interpretation and reduces the risk that apparent differences reflect missingness rather than signal.

Variables that recur across thresholded and regularised models are the strongest candidates for a common reporting core in future field trials because they appear to carry signal that is portable across sites and modelling choices. In this study, those variables were most often soil nitrogen, soil acidity, fertiliser context, biochar carbon, and application rate. Variables whose centrality or connectivity shifts sharply across specifications remain valuable, but they are most informative when measured alongside that core rather than interpreted in isolation. In that sense, robustness analysis is not only a statistical check, but also a guide to which measurements are most likely to support cumulative inference across studies. For exploratory ecological networks, the practical aim is less to catalogue every possible edge than to identify the subset of recurring patterns that can support cross-site comparison and justify more targeted mechanistic or predictive follow-up (Golino and Epskamp, 2017). For a single, well-controlled field experiment, these networks are therefore best used to prioritise variables and frame hypotheses, not to substitute for experimental inference (Dablander and Hinne, 2019).

4.3. Current limitations and targeted future directions

Several limitations arise from the structure of the published evidence. Many trials report soil and biochar properties as study descriptors rather than as paired control and treatment values, so these variables contextualise emission lnRRs rather than functioning as treatment-response effect sizes. Reporting of dispersion and sample size is also uneven across variables, which limits formal uncertainty propagation for the full node set. In addition, pairwise missingness means that edge-specific joint coverage varies across the network, and fragmentation after thresholding can reflect both weak association structure and limited joint reporting. These constraints do not invalidate descriptive network synthesis, but they set expectations for what can be interpreted and why stability-oriented checks are needed.

The robustness checks strengthen confidence in the backbone of the network, but they do not remove the main limitations of the evidence base. The fact that observed association strength and density exceeded null expectations argues against the recovered structure being a simple by-product of missingness or sample size alone. At the same time, lower agreement between marginal correlation networks and regularised partial-correlation networks, especially in rice, short-duration, and some high-rainfall strata, shows that many weaker peripheral links are not yet portable across modelling choices. Those associations are therefore better treated as provisional signals for follow-up than as settled ecological relationships.

Harmonised reporting of a minimal measurement set, including dispersion and sample size, would increase joint coverage and reduce node-set differences across contexts. Designs that report core soil variables in both control and treatment conditions, alongside emissions, would allow a clearer separation between contextual descriptors and treatment-responsive effect sizes, and would enable stronger multivariate modelling beyond descriptive association structure. Longer field durations and repeated measurements would allow direct evaluation of whether multivariate organisation is stable or rewires as biochar ages and management changes (Blonder et al., 2012). As the available evidence base grows, leave-one-study-out analyses, broader regularisation sensitivity tests, and repeated validation across contexts will help separate recurrent ecological structure from study-specific covariance patterns, sparse reporting, and model-dependent edge retention (Epskamp et al., 2018).

Overall, the stratified network approach provides a structured way to organise multi-domain field evidence while keeping uncertainty explicit. It highlights the part of the multivariate structure most likely to generalise across thresholds, estimators, and missingness-aware null models, while also showing where limited joint coverage and model sensitivity still constrain inference. That distinction is directly relevant for designing monitoring programmes that aim to compare biochar outcomes across contexts.

5. Conclusion

Field trials continue to report variable N_2O, CH_4, and CO_2 outcomes under biochar amendment, and those outcomes are measured alongside an uneven set of soil, management, biochar, and microbial descriptors. This study reorganised that evidence as stratified association networks, using lnRR effect sizes for emissions and treating other variables as contextual descriptors. Across strata, retained association structure ranged from networks that remained largely connected to networks that fragmented at the operating threshold, which sets clear limits on when path-based summaries and centrality measures represent the full variable set. Despite context dependence and uneven reporting, a consistent pattern emerged. When available and connected, soil pH, nitrogen-related descriptors, and biochar application rate often sit in well-connected regions of the retained graphs. Conditioning and resampling further reduced attention to a narrower subset of reproducible links, including repeated support for the bRate-spH association in strata where both variables were available. The framework remains descriptive, but it provides a practical basis for identifying core indicators that are most defensible for stratified monitoring and for prioritising contexts where cross-domain interpretation is better supported by the published data. More standardised co-measurement, fuller reporting of uncertainty, and longer-duration trials would strengthen future tests of whether the recurring features identified here generalise across sites and management practices.

CRediT authorship contribution statement

Sudhir Yadav: Writing – review & editing, Supervision, Conceptualization. **Moreira Bruno Rafael de Almeida:** Writing – review & editing, Writing – original draft, Visualization, Methodology, Investigation, Formal analysis, Conceptualization. **Jinze Bai:** Writing – review & editing, Writing – original draft, Visualization, Investigation, Data curation.

Declaration of Generative AI and AI-assisted technologies in the writing process

During the preparation of this work the authors utilised Microsoft Copilot, an AI-assisted technology, to improve the overall readability of the manuscript. After utilising this tool/service, the authors reviewed and edited the content as necessary. As a result, they take full responsibility for the accuracy, integrity, and scientific rigor of the publication.

Declaration of Competing Interest

The authors declare that they have no known competing financial interests or personal relationships that could have appeared to influence the work reported in this article.

Acknowledgements

The authors gratefully acknowledge support from the University of Queensland (UQ), which hosted Jinze Bai through a visiting scholar program. Additionally, the authors thank Northwest A&F University for providing Jinze Bai with scholarship funding to support this collaborative research effort.

Appendix A. Supporting information

Supplementary data associated with this article can be found in the online version at doi:10.1016/j.still.2026.107193.

Data availability

Data will be made available on request.

References

Arthur, R., 2025. Correlation and autocorrelation of data on complex networks. EPJ Data Sci. 14.
Bai, J., De Almeida Moreira, B.R., Bai, Y., Nadar, C.G., Feng, Y., Yadav, S., 2025. Assessing biochar's impact on greenhouse gas emissions, microbial biomass, and enzyme activities in agricultural soils through meta-analysis and machine learning. Sci. Total Environ. 963.
Bai, X., Huang, Y., Ren, W., Coyne, M., Jacinthe, P.A., Tao, B., Hui, D., Yang, J., Matocha, C., 2019. Responses of soil carbon sequestration to climate-smart agriculture practices: a meta-analysis. Glob. Change Biol. 25, 2591–2606.
Bauwens, T., Schraven, D., Drewing, E., Radtke, J., Holstenkamp, L., Gotchev, B., Yildiz, Ö., 2022. Conceptualizing community in energy systems: a systematic review of 183 definitions. Renew. Sustain. Energy Rev. 156.
Blonder, B., Wey, T.W., Dornhaus, A., James, R., Sih, A., 2012. Temporal dynamics and network analysis. Methods Ecol. Evol. 3, 958–972.
Bolan, S., Hou, D., Wang, L., Hale, L., Egamberdieva, D., Tammeorg, P., Li, R., Wang, B., Xu, J., Wang, T., Sun, H., Padhye, L.P., Wang, H., Siddique, K.H.M., Rinklebe, J., Kirkham, M.B., Bolan, N., 2023. The potential of biochar as a microbial carrier for agricultural and environmental applications. Sci. Total Environ. 886.
Borchard, N., Schirrmann, M., Cayuela, M.L., Kammann, C., Wrage-Mönnig, N., Estavillo, J.M., Fuertes-Mendizábal, T., Sigua, G., Spokas, K., Ippolito, J.A., Novak, J., 2019. Biochar, soil and land-use interactions that reduce nitrate leaching and N2O emissions: a meta-analysis. Sci. Total Environ. 651, 2354–2364.
Borsboom, D., Deserno, M.K., Rhemtulla, M., Epskamp, S., Fried, E.I., McNally, R.J., Robinaugh, D.J., Perugini, M., Dalege, J., Costantini, G., Isvoranu, A.M., Wysocki, A. C., van Borkulo, C.D., van Bork, R., Waldorp, L.J., 2021. Network analysis of multivariate data in psychological science. Nat. Rev. Methods Prim. 1.
Cayuela, M.L., Sánchez-Monedero, M.A., Roig, A., Hanley, K., Enders, A., Lehmann, J., 2013. Biochar and denitrification in soils: when, how much and why does biochar reduce N2O emissions? Sci. Rep. 3.
Chagas, J.K.M., Figueiredo, C.C.D., Ramos, M.L.G., 2022. Biochar increases soil carbon pools: evidence from a global meta-analysis. J. Environ. Manag. 305.
Dablander, F., Hinne, M., 2019. Node centrality measures are a poor substitute for causal inference. Sci. Rep. 9.
Epskamp, S., 2020. Psychometric network models from time-series and panel data. Psychometrika 85, 206–231.
Epskamp, S., Fried, E.I., 2018. A tutorial on regularized partial correlation networks. Psychol. Methods 23, 617–634.
Epskamp, S., Cramer, A.O.J., Waldorp, L.J., Schmittmann, V.D., Borsboom, D., 2012. Qgraph: network visualizations of relationships in psychometric data. J. Stat. Softw. 48.
Epskamp, S., Borsboom, D., Fried, E.I., 2018. Estimating psychological networks and their accuracy: a tutorial paper. Behav. Res. Methods 50, 195–212.
Fruchterman, T.M.J., Reingold, E.M., 1991. Graph drawing by force-directed placement. Softw. Pract. Exp. 21, 1129–1164.
Golino, H.F., Epskamp, S., 2017. Exploratory graph analysis: a new approach for estimating the number of dimensions in psychological research. Plos One 12.
Hedges, L.V., Gurevitch, J., Curtis, P.S., 1999. The meta-analysis of response ratios in experimental ecology. Ecology 80, 1150–1156.
Hénault, C., Bourennane, H., Ayzac, A., Ratié, C., Saby, N.P.A., Cohan, J.P., Eglin, T., Gall, C.L., 2019. Management of soil pH promotes nitrous oxide reduction and thus mitigates soil emissions of this greenhouse gas. Sci. Rep. 9.
Hu, A., Choi, M., Tanentzap, A.J., Liu, J., Jang, K.S., Lennon, J.T., Liu, Y., Soininen, J., Lu, X., Zhang, Y., Shen, J., Wang, J., 2022. Ecological networks of dissolved organic matter and microorganisms under global change. Nat. Commun. 13.
Jia, X., Yan, W., Yang, J., Chen, W., Ma, H., Chen, X., Liu, J., Zhong, Y., Shangguan, Z., 2023. Global patterns and controls of soil greenhouse gas fluxes and crop yield under biochar application. Land Degrad. Dev. 34, 5622–5634.
Jiang, Y., Qian, H.Y., Huang, S., Zhang, X.Y., Wang, L., Zhang, L., Shen, M.X., Xiao, X.P., Chen, F., Zhang, H.L., Lu, C.Y., Li, C., Zhang, J., Deng, A.X., van Groenigen, K.J., Zhang, W.J., 2019. Acclimation of methane emissions from rice paddy fields to straw addition. Sci. Adv. 5.
Kabir, E., Kim, K.H., Kwon, E.E., 2023. Biochar as a tool for the improvement of soil and environment. Front. Environ. Sci. 11.
Kerner, P., Struhs, E., Mirkouei, A., Aho, K., Lohse, K.A., Dungan, R.S., You, Y., 2023. Microbial responses to biochar soil amendment and influential factors: a three-level meta-analysis. Environ. Sci. Technol. 57, 19838–19848.
Khalifah, S., Foltz, M.E., 2024. The ratio of denitrification end-products were influenced by soil pH and clay content across different texture classes in Oklahoma soils. Front. Soil Sci. 4.
Khan, S., Irshad, S., Mehmood, K., Hasnain, Z., Nawaz, M., Rais, A., Gul, S., Wahid, M.A., Hashem, A., Abd_Allah, E.F., Ibrar, D., 2024. Biochar production and characteristics, its impacts on soil health, crop production, and yield enhancement: a review. Plants 13.
Lehmann, J., Bossio, D.A., Kögel-Knabner, I., Rillig, M.C., 2020. The concept and future prospects of soil health. Nat. Rev. Earth Environ. 1, 544–553.
Lehmann, J., Cowie, A., Masiello, C.A., Kammann, C., Woolf, D., Amonette, J.E., Cayuela, M.L., Camps-Arbestain, M., Whitman, T., 2021. Biochar in climate change mitigation. Nat. Geosci. 14, 883–892.

Liao, X., Chen, Y., Hu, J., Zhang, C., Mao, S., Ruan, H., Malghani, S., 2025. Effects of fresh and aged biochar on N2O emission from a poplar plantation soil. Pedosphere 35, 435–447.

Liberati, A., Altman, D.G., Tetzlaff, J., Mulrow, C., Gøtzsche, P.C., Ioannidis, J.P.A., Clarke, M., Devereaux, P.J., Kleijnen, J., Moher, D., 2009. The PRISMA statement for reporting systematic reviews and meta-analyses of studies that evaluate health care interventions: explanation and elaboration. Ital. J. Public Health 6, 354–391.

Liu, X., Dai, X.Q., Yang, F.T., Meng, S.W., Wang, H.M., 2023. CH4 emissions from a double-cropping rice field in subtropical China over seven years. Agr. For. Meteor. 339.

López-Aizpún, M., Horrocks, C.A., Charteris, A.F., Marsden, K.A., Ciganda, V.S., Evans, J. R., Chadwick, D.R., Cárdenas, L.M., 2020. Meta-analysis of global livestock urine-derived nitrous oxide emissions from agricultural soils. Glob. Change Biol. 26, 2002–2013.

Masson-Delmotte, V., Pörtner, H.O., Skea, J., Zhai, P., Roberts, D., Shukla, P.R., Pirani, A., Moufouma-Okia, W., Péan, C., Pidcock, R., Connors, S., Matthews, J.B.R., Chen, Y., Zhou, X., Gomis, M.I., Lonnoy, E., Maycock, T., Tignor, M., Waterfield, T., 2022. Global warming of 1.5°C: An IPCC Special Report on the impacts of global warming of 1.5°C above pre-industrial levels and related global greenhouse gas emission pathways, in the context of strengthening the global response to the threat of climate change, sustainable development, and efforts to eradicate poverty.

Morton, J.T., Marotz, C., Washburne, A., Silverman, J., Zaramela, L.S., Edlund, A., Zengler, K., Knight, R., 2019. Establishing microbial composition measurement standards with reference frames. Nat. Commun. 10.

Muratori, M., Bauer, N., Rose, S.K., Wise, M., Daioglou, V., Cui, Y., Kato, E., Gidden, M., Strefler, J., Fujimori, S., Sands, R.D., van Vuuren, D.P., Weyant, J., 2020. EMF-33 insights on bioenergy with carbon capture and storage (BECCS). Clim. Change 163, 1621–1637.

Opsahl, T., Agneessens, F., Skvoretz, J., 2010. Node centrality in weighted networks: generalizing degree and shortest paths. Soc. Netw. 32, 245–251.

Schmidt, H.P., Kammann, C., Hagemann, N., Leifeld, J., Bucheli, T.D., Sánchez Monedero, M.A., Cayuela, M.L., 2021. Biochar in agriculture – a systematic review of 26 global meta-analyses. GCB Bioenergy 13, 1708–1730.

Singh, D., Lenka, S., Kanwar, R.S., Yadav, S.S., Saha, M., Sarkar, A., Yadav, D.K., Vassanda Coumar, M., Lenka, N.K., Adhikari, T., Jadon, P., Gami, V., 2024. Drivers of greenhouse gas emissions in agricultural soils: the effect of residue management and soil type. Front. Environ. Sci. 12.

Tian, H.Q., Xu, R.T., Canadell, J.G., Thompson, R.L., Winiwarter, W., Suntharalingam, P., Davidson, E.A., Ciais, P., Jackson, R.B., Janssens-Maenhout, G., Prather, M.J., Regnier, P., Pan, N.Q., Pan, S.F., Peters, G.P., Shi, H., Tubiello, F.N., Zaehle, S., Zhou, F., Arneth, A., Battaglia, G., Berthet, S., Bopp, L., Bouwman, A.F., Buitenhuis, E.T., Chang, J.F., Chipperfield, M.P., Dangal, S.R.S., Dlugokencky, E., Elkins, J.W., Eyre, B.D., Fu, B.J., Hall, B., Ito, A., Joos, F., Krummel, P.B., Landolfi, A., Laruelle, G.G., Lauerwald, R., Li, W., Lienert, S., Maavara, T., MacLeod, M., Millet, D.B., Olin, S., Patra, P.K., Prinn, R.G., Raymond, P.A., Ruiz, D. J., van der Werf, G.R., Vuichard, N., Wang, J.J., Weiss, R.F., Wells, K.C., Wilson, C., Yang, J., Yao, Y.Z., 2020. A comprehensive quantification of global nitrous oxide sources and sinks. NATURE 586, 248.

Tian, J.H., Dunfield, K., Condron, L., 2024. Biological cycling of nitrogen and phosphorus in soils. Plant Soil 498, 1–4.

Weng, Z.H., Cowie, A.L., 2025. Estimates vary but credible evidence points to gigaton-scale climate change mitigation potential of biochar. Commun. Earth Environ. 6.

Williams, D.R., 2022. Learning to live with sampling variability: expected replicability in partial correlation networks. Psychol. Methods 27, 606–621.

Yang, J., Li, G., Qian, Y., Yang, Y., Zhang, F., 2018. Microbial functional gene patterns related to soil greenhouse gas emissions in oil contaminated areas. Sci. Total Environ. 628-629, 94–102.

Yang, M., Wang, H., Wei, Z., Wang, S., Wen, J.R., 2024. Efficient algorithms for personalized pagerank computation: a survey. IEEE Trans. Knowl. Data Eng. 36, 4582–4602.